

**Original Research Article****Rapid and Sensitive Quantification of Isoproterenol in the Presence of Theophylline by CuO Nanoflowers Modified Electrochemical Sensor**Maryam Ebrahimi¹, Hadi Beitollahi^{2,*}¹Department of Chemistry, Graduate University of Advanced Technology, Kerman, Iran²Environment Department, Institute of Science and High Technology and Environmental Sciences, Graduate University of Advanced Technology, Kerman, Iran**ARTICLE INFO****Article history**

Submitted: 2021-05-24

Revised: 2021-06-27

Accepted: 2021-08-04

Manuscript ID: CHEMM-2105-1341

Checked for Plagiarism: Yes

Language Editor:

Dr. Behrouz Jamavandi

Editor who approved publication:

Dr. Hasan Karimi Maleh,

DOI: 10.22034/chemm.2021.134961**KEY WORDS**

Glassy carbon electrode

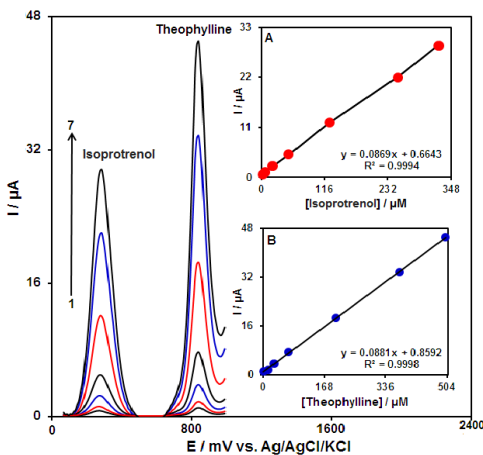
CuO nanoflowers

Isoproterenol

Theophylline

ABSTRACT

Isoproterenol is an important catecholamine-based drug that is widely used in the treatment of heart disease. The present paper introduced one of the new modifications for the surfaces of glassy carbon electrodes (GCEs) using the CuO nanoflowers (CuO NFs) for determination of isoproterenol. Electrochemical properties of the CuO NFs/GCE for detecting isoproterenol were tested using the cyclic voltammetry (CV), chronoamperometry (CHA) as well as differential pulse voltammetry (DPV). Electrochemical studies demonstrated an efficient isoproterenol oxidation, with enhanced peak current from 2.9 μ A to about 10.0 μ A (3.4% increase) and decreased peak potential from 500 mV to about 300 mV. The linear response for the determination of isoproterenol was obtained in ranges for concentrations between 0.3 and 450.0 μ M under the most proper conditions and the limit of detection (LOD) equaled 0.09 μ M. Also, the modified electrode is utilized for simultaneously determining isoproterenol and theophylline using DPV. The proposed CuO NFs/GCE sensor was effectively employed for the isoproterenol and theophylline detection in the isoproterenol ampoule and urine samples.

GRAPHICAL ABSTRACT

* Corresponding author: Hadi Beitollahi

✉ E-mail: h.beitollahi@yahoo.com

© 2021 by SPC (Sami Publishing Company)

Introduction

Isoproterenol has been proposed as one of the catecholamine medications. Being a nonselective beta-adrenergic agonist, it has the same structure as adrenaline (epinephrine). Actually, isopropyl amino group in isoproterenol makes it selective for β -receptors. The free catechol hydroxy groups keep it susceptible to enzymatic metabolism. Isoproterenol is used for the treatment of bradycardia (slow heart rate), heart block, rarely for asthma, glaucoma and as styptic. Nevertheless, the excess of the drug may cause heart failure and arrhythmias [1,2].

Theophylline (TP), also known as 1,3-dimethylxanthine, has been considered as a methylated xanthine that has relaxing impacts on the smooth muscle of the lung airways. It is capable of causing various physiological impacts such as relaxation of the bronchial muscle, enhancement of the gastric acid secretion, and stimulation of the central nervous system (CNS). This compound has been introduced as one of the conventional medications for chronic asthma [3] with the effects on the range of concentrations from 5–20 $\mu\text{g}/\text{mL}$ (55–110 μM). Over 20 $\mu\text{g}/\text{mL}$, it has been found that theophylline may result in ranges between moderate and severe condition, including fever, arrhythmia, insomnia, dehydration, heartburn tachycardia, coma, anorexia, and cardiac and respiratory arrest [4]. Because of this, it is crucial to have a method which can detect theophylline in a simple, rapid, and efficient way [4].

Analytical methods have attracted more attention in recent years in separation and detection systems [5-11]. Experts in the field have employed a variety procedures to detect theophylline and isoproterenol in biological fluids, foodstuff, and pharmaceutical compounds that contain flow Injection spectrophotometric [12], high-performance liquid chromatography (HPLC) [13,14], capillary electrophoresis [15], chemiluminescence [16,17], surface-enhanced Raman scattering [18], gas chromatography-mass spectrometry [19], and electrochemical methods [20-23]. Most of these techniques have been recognized to be laborious that require

extraction, costly instruments, as well as intensive solvent-usage. Amongst diverse analytical procedures, the electrochemical techniques have been identified as an attractive technique because of higher selectivity and sensitivity, simplified construction and rapid time for responses [24-30].

The chemical modifications of the inert substrate electrode with modifiers have offered considerable merits in designing and developing electrochemical sensors [31-38]. During the operation, active sites of the redox shuttle the electrons between the analyte solution and substrate electrode followed by a remarkable decline in the over-potential of activation. Another merit considered for the chemically modified electrodes has been introduced to their lower susceptibility to the surface fouling and oxide formation in comparison with the inert substrate electrodes [38].

The unique properties of nanoparticles make them an extremely valuable modifying material, being used for electrochemical applications [39-42].

Recently, nanomaterials have some uses in fabricating sensors because of the ratio of larger surface areas to volume, higher mass transference, high electrical conductivity as well as fast rate in electro-catalysis [43-50]. Researchers have also addressed numerous noble metals like Au, Pt and Pd and their composites such as Au-Pd, Pt-Au, Pt-Pd, and so on for electrochemical sensing [51-53]. However, the cost of these metals has encouraged to explore the possibility of metal oxides such as CuO, NiO, ZnO, Cu₂O, MnO₂, Fe₂O₃, SnO₂ and Ag₂O for developing low-cost electrochemical sensors [54-56]. Among them, CuO nanostructure; for example, nanowires, nanorods, nanoflowers, and so forth have a widespread utilization to design cheap electrochemical sensors because of its acceptable electro-chemical and electrocatalytic features as well as easy availability [57-59]. Researchers have commonly employed the intrinsically p-type semi-conductor CuO with a bandgap of nearly 1.2 eV in the lithium-ion batteries, photo-electric instruments, gas sensors

as well as electrochemical sensors because of the respective attractive optical and electrical features [60-63].

In this paper, a convenient, economical and simple method was used to fabricate CuO NFs/GCE as one of the novel electrodes in electrocatalysis and detection of isoproterenol. In the next step, we assessed analytical function of the modified electrodes for quantifying isoproterenol in the presence of theophylline. Moreover, our electro-chemical sensor has been applied to detect theophylline and isoproterenol in real samples.

Material and methods

Chemicals and apparatus

In this step, electrochemical measurements have been done using an Auto-lab potentiostat/galvanostat. Measurements have been performed at room temperature, with a single component 3-electrode cell that had a platinum auxiliary electrode and an Ag/AgCl (3 M KCl) reference electrode. CuO NFs/GCE has been used as the working electrode and a Metrohm 827 pH-meter has been used for controlling the pH of solutions. Each chemical has been of analytical reagent grade that has been bought from Merck Company in Darmstadt, Germany. In addition, we applied doubly distilled-water. Isoproterenol, theophylline and all other reagents have been of analytical grade and were obtained from Merck chemical company.

Modification of GCE by CuO NFs

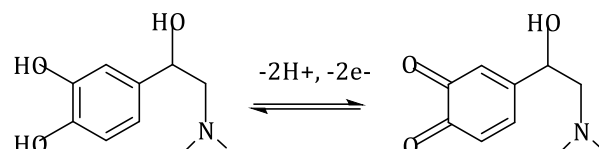
For preparing the CuO NFs modified GCE, 1mg of CuO NFs was dispersed in 1 mL distilled water and ultrasonicated for nearly thirty minutes. Then 4 μ L of the suspension has been coated on the GCE surface and finally dried at the room temperature.

Electrochemical behavior of the isoproterenol on the CuO NFs/GCE

The effects of the pH of solution on the oxidation responses of CuO NFs/GCE E for 100.0 μ M isoproterenol was carefully investigated by CV in 0.1 M PBS in various pH-values (2.0 - 9.0). It is notable that under pH 7.0 of PBS, we observed

the best voltammetric responses; i.e., the largest peak current. Finally, we chose pH 7.0 for other analytical experimentations.

The oxidation mechanism of isoproterenol is presented in Scheme 1.



Scheme 1: Mechanism of isoproterenol electrooxidation

The cyclic voltammograms (CVs) recorded by bare GCE, as shown in Figure 1, curve a, and CuO NFs/GCE as shown in curve b, were carried out between using 50 mVs⁻¹ scan rate in 0.1M PBS at a pH of 7.0, including 100.0 μ M isoproterenol. The anodic peak potential for isoproterenol oxidation at the bare GCE is \sim 500 mV in comparison to 300 mV for on the CuO NFs/GCE. Moreover, the current value increased in modified electrode (CuO NFs/GCE) which revealed that the CuO NFs/GCE had electrocatalytic behavior to the isoproterenol oxidation.

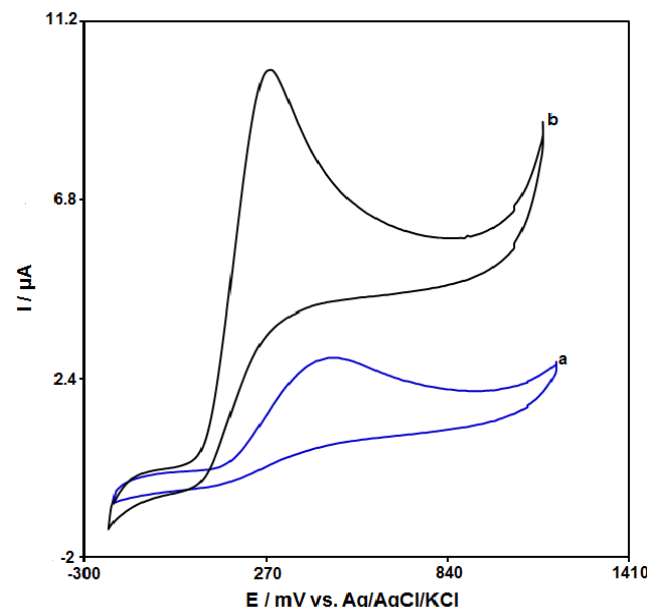


Figure 1: CVs of (a) bare GCE and (b) CuO NFs/GCE in 100.0 μ M isoproterenol at the scan rate 50 mVs⁻¹

Result and Dissection

Effect of scan rate

We determined the effects of the potent scan rate on the current of isoproterenol oxidation Figure 2. Enhancing the potential scan rate elevated the peak current. Additionally, the oxidation process

was controlled by diffusion that is due to the linear dependence of I_p on the $v^{1/2}$ within a wider range between 10 and 900 mVs⁻¹.

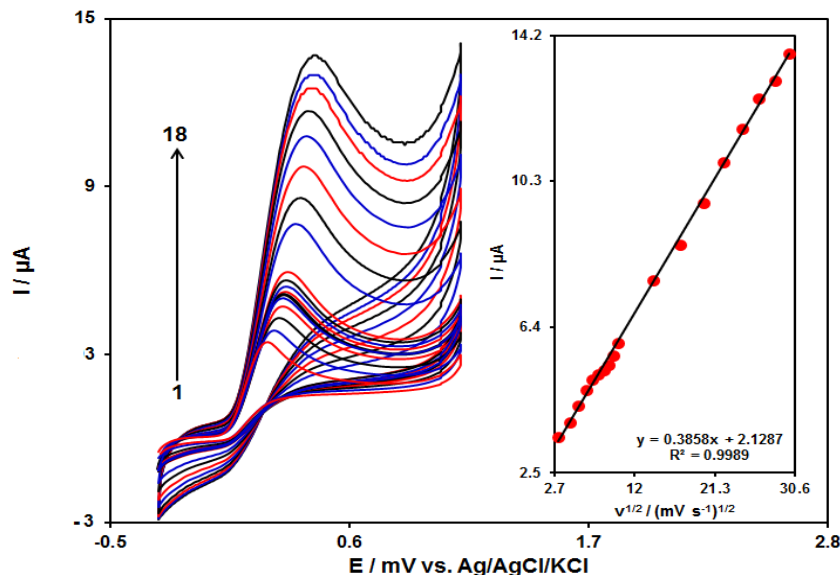


Figure 2: (A) CVs of CuO NFs/GCE in 0.1 M PBS containing 50.0 μ M of isoproterenol various scan rates; numbers 1–18 correspond to 10, 20, 30, 40, 50, 60, 70, 80, 90, 100, 200, 300, 400, 500, 600, 700, 800 and 900 mV s⁻¹. Inset: Variation of I_p vs. $v^{1/2}$

We used data from the ascending section; that is, Tafel region) of the current–voltage curve achieved at 10 mVs⁻¹ (Figure 3) for plotting another Tafel. Moreover, Tafel region of the current potential curve would be impacted by the

kinetic of the electron transfer of the electrode reaction. According to the findings, Tafel slope = 0.1047 V, reflecting a 1 electron (Figure 3) rate-determining step for the electrode process [64] for the charge transfer coefficient (α) equal to 0.44.

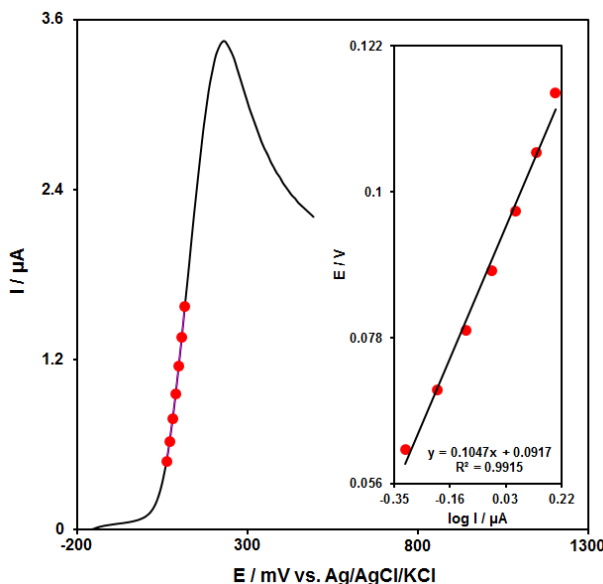


Figure 3: LSV (at 10 mV s⁻¹) of CuO NFs/GCE in 50.0 μ M isoproterenol. The points are the data used in the Tafel plot (inset)

Chronoamperometric analysis

With the confirmation of diffusion process during the isoproterenol oxidation process on the

surface of CuO NFs/GCE, the chronoamperometric method with applied potential of 0.35 V has been employed for

determining diffusion coefficient (D) of isoproterenol (Figure 4). Experimental outputs of I versus $t^{-1/2}$ were drawn by Figure 4A, with the best fits for various concentrations of isoproterenol. In the next step, we plotted final

slopes that corresponded to the straight lines in Figure 4A, plotted against isoproterenol concentration (Fig. 4B). Finally, mean value of D was computed $1.5 \times 10^{-6} \text{ cm}^2/\text{s}$ based on the Cottrell equation and final slope [64].

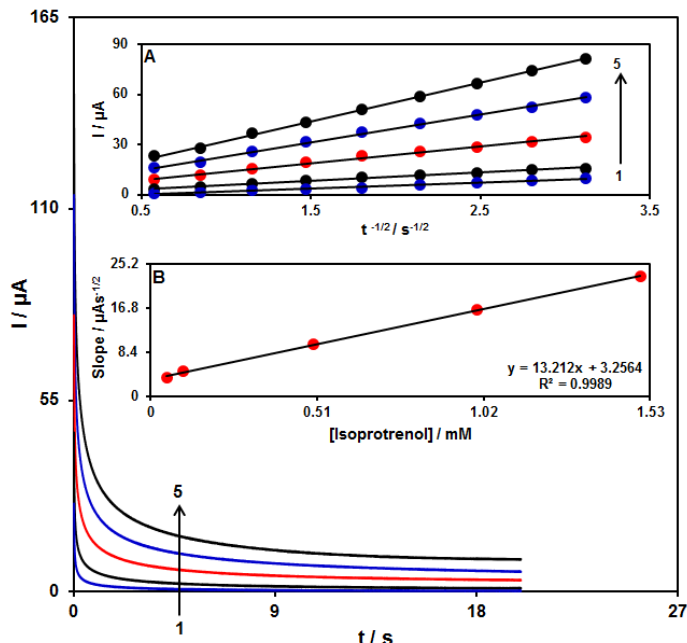


Figure 4: Chronoamperograms obtained at CuO NFs/GCE for different concentration of isoproterenol. The numbers 1–5 correspond to 0.05, 0.1, 0.5, 1.0 and 1.5 mM of isoproterenol. Insets: (A) Plots of I vs. $t^{-1/2}$ obtained from chronoamperograms 1–5. (B) Plot of the slope of the straight lines against isoproterenol concentration

Calibration plot and limit of detection

In this step, we used DPV for investigating voltammetric sensor of CuO NFs/GCE towards detecting isoproterenol detection (Step potential=0.01 V and pulse amplitude=0.025 V). Figure 5 showed the differential pulse voltammograms of isoproterenol with diverse concentrations in 0.1 mol L⁻¹ PBS at a pH of 7.0.

We showed in Figure 5 (inset) linear enhancement of the oxidation current with isoproterenol concentrations in ranges from 0.3–450.0 μM . Moreover, linear regression equation was expressed as $I_{\text{pa}} = 0.0873C(\mu\text{M}) + 0.5548$ ($R^2 = 0.9997$) and limit of detection (LOD) of isoproterenol equaled 0.09 μM .

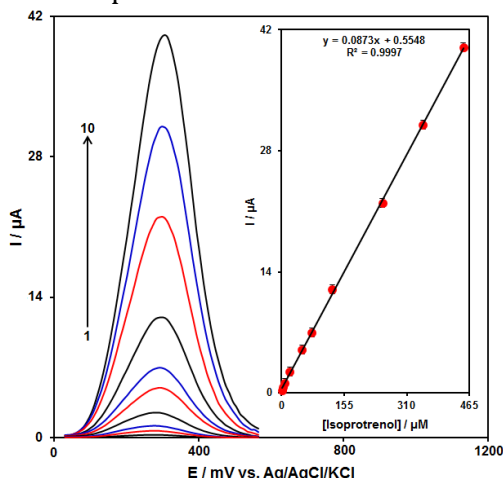


Figure 5: DPVs of CuO NFs/GCE for containing different concentrations of isoproterenol. Numbers 1–10 correspond to 0.3, 2.5, 7.5, 20.0, 50.0, 75.0, 125.0, 250.0, 350.0, and 450.0 μM of isoproterenol. Insets: plot of the electrocatalytic peak current as a function of isoproterenol concentration in the range of 0.3–450.0 μM

Table 1: Comparison of the efficiency of some modified electrodes used in the electrooxidation of isoproterenol

Entry	Limit of detection	Linear range	Methods	Electrochemical sensor	Ref.
1	1.9 μM	8.0–50 μM	SWV	GO-CB-PEDOT:PSS/GCE	20
2	0.082 μM	0.1–900.0 μM	DPV	GCE/AuNPs/DPB	21
3	0.47 μM	0.5–1000.0 μM	DPV	CD-TMCPE	65
4	0.47 μM	0.8–570.0 μM	SWV	PGRMMWCNTPE	66
5	$1.60 \times 10^{-7} \text{ M}$	2.0×10^{-6} – $6.0 \times 10^{-5} \text{ M}$	CV	poly(1-methylpyrrole)-DNA/GCE	67
6	0.09 μM	0.3–450.0 μM	DPV	CuO NFs/GCE	This work

Simultaneous Determination of isoproterenol and theophylline

The present research mainly aimed at the simultaneous detection of both isoproterenol and theophylline. Therefore, we simultaneously changed the concentration of isoproterenol and theophylline, and recorded DPV (Step potential=0.01 V and pulse amplitude=0.025 V). According to the voltammetric outputs, we observed the completely organized anodic peaks at the potential equal to 290 and 840 mV, which corresponded to isoproterenol and theophylline

oxidation, suggesting the feasibility of simultaneous detection of the compounds (Figure 6). Moreover, sensitivity of the modified electrode for oxidizing isoproterenol equaled $0.0869 \mu\text{A } \mu\text{M}^{-1}$ that was highly close to the value observed in the absence of theophylline ($0.0884 \mu\text{A } \mu\text{M}^{-1}$, Figure 5), revealing independence of the oxidation processes of the compounds at the CuO NFs/GCE as well as feasible simultaneous detection of the mixtures without any significant interference.

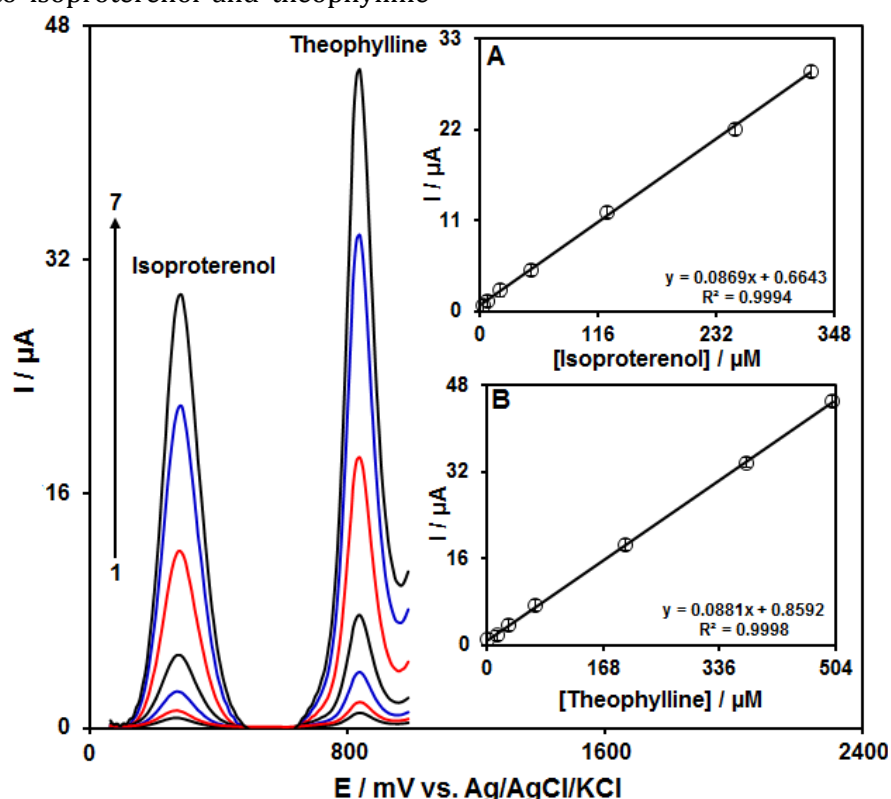


Figure 6: DPVs of CuO NFs/GCE for different concentrations of isoproterenol and theophylline. Numbers 1–7 correspond to: 2.5+1.0, 7.5+15.0, 20.0+30.0, 50.0+70.0, 125.0+200.0, 250.0+375.0 and 325.0+500.0 respectively. Insets: (A) plots of I_p vs. isoproterenol concentrations and (B) plot of I_p vs. theophylline concentrations

Determination of isoproterenol and theophylline in isoproterenol ampoule and urine samples

We used CuO NFs/GCE to evaluate its practical application for determining isoproterenol and

theophylline in isoproterenol ampoule and urine samples. DPV response of the samples was identified by some experiments and then isoproterenol and theophylline concentrations were added. In the next stage, we used standard

addition for quantitative analysis of solutions so recovery ranged from 97.5%-103.3% (Table 2). Outputs reflected the possible feasibility of our new electrode in the real samples with acceptable confidence level.

Table 2: The application of CuO NFs/GCE for simultaneous determination of isoproterenol and theophylline in isoproterenol ampoule and urine samples (n =5)

Sample	Spiked (μM)		Found (μM)		Recovery (%)		(%R.S.D.)	
	Isoproterenol	Theophylline	Isoproterenol	Theophylline	Isoproterenol	Theophylline	Isoproterenol	Theophylline
Isoproterenol Ampoule	0	0	5.0	-	-	-	3.3	-
	2.5	5.0	7.4	5.1	98.7	102.0	1.7	3.1
	5.0	10.0	10.3	9.9	103.0	99.0	2.8	2.4
	7.5	15.0	12.4	15.5	99.2	103.3	2.9	1.9
	12.5	20.0	17.6	19.7	100.6	98.5	2.4	2.3
Urine	0	0	-	-	-	-	-	-
	5.0	7.5	5.1	7.4	103.0	98.7	3.4	1.8
	10.0	12.5	9.9	13.0	99.0	104.0	3.2	2.9
	15.0	17.5	15.4	17.0	102.7	97.1	2.7	3.5
	20.0	22.5	19.5	22.6	97.5	100.4	1.9	3.5

Conclusion

We demonstrated CuO NFs/GCE fabrication and its utilization in simultaneous detection of isoproterenol and theophylline. The electrode showed excellent sensitivity for isoproterenol signal. CuO NFs/GCE showed good electrocatalytic activity for analysis of isoproterenol in the concentration range 0.3-450.0 μM with limit of detection 0.09 μM . Finally, the CuO NFs/GCE showed good ability for analysis of isoproterenol and theophylline in the real samples.

Funding

This research did not receive any specific grant from funding agencies in the public, commercial, or not-for-profit sectors.

Authors' contributions

All authors contributed toward data analysis, drafting and revising the paper and agreed to be responsible for all the aspects of this work.

Conflict of Interest

We have no conflicts of interest to disclose.

References

- [1]. Arteaga de Murphy C., Ferro-Flores G., Villanueva-Sanchez O., Murphy-Stack E., Pedraza-

López M., Meléndez-Alafort L., Molina-Trinidad E., *Int. J. Pharm.*, 2002, **233**:29 [[Crossref](#)], [[Google Scholar](#)], [[Publisher](#)]

[2]. Wang J., Li Y., Li C., Zeng X., Tang W., Chen X., *Microchim. Acta*, 2017, **184**:2999 [[Crossref](#)], [[Google Scholar](#)], [[Publisher](#)]

[3]. Pal R., Chaudhary M.J., Tiwari P.C., Babu S., Pant K., *Int. Immunopharmacol.*, 2015, **29**:854 [[Crossref](#)], [[Google Scholar](#)], [[Publisher](#)]

[4]. Hu L.Y., Chen L.X., Liu M.T., Wang A.J., Wu L.J., Feng J.J., *J. Colloid Interface Sci.*, 2017, **493**:94 [[Crossref](#)], [[Google Scholar](#)], [[Publisher](#)]

[5]. Tajik S., Taher M.A., *Desalination*, 2011: **278**:57 [[Crossref](#)], [[Google Scholar](#)], [[Publisher](#)]

[6]. Beytollahi A., *Eurasian Chem. Commun.*, 2020, **2**:916 [[Crossref](#)], [[Google Scholar](#)], [[Publisher](#)]

[7]. Tajik S., Taher M.A., *Microchim. Acta*, 2011, **173**:249 [[Crossref](#)], [[Google Scholar](#)], [[Publisher](#)]

[8]. Karimi-Maleh H., Arotiba O.A., *J. Colloid Interface Sci.*, 2020, **560**:208 [[Crossref](#)], [[Google Scholar](#)], [[Publisher](#)]

[9]. Tajik S., Taher M.A., Sheikhshoae I., *J. AOAC Int.*, 2013, **96**:204 [[Crossref](#)], [[Google Scholar](#)], [[Publisher](#)]

[10]. Tahernejad-Javazmi F., Shabani-Nooshabadi M., Karimi-Maleh H., *Compos. Part B-*

- Eng., 2019, **172**:666 [[Crossref](#)], [[Google Scholar](#)], [[Publisher](#)]
- [11]. Beytollahi A., *Chem. Methodol.* 2020, **5**: 114 [[Crossref](#)], [[Google Scholar](#)], [[Publisher](#)]
- [12]. Bonifácio V.G., Marcolino-Júnior L.H., Fatibello-Filho O., *Anal. Lett.*, 2004, **37**:2111 [[Crossref](#)], [[Google Scholar](#)], [[Publisher](#)]
- [13]. Kishimoto Y., Ohgitani S., Yamatodani A., Kuro M., Okumura F., *J. Chromatogr. B Biomed. Appl.*, 1982, **231**:121 [[Crossref](#)], [[Google Scholar](#)], [[Publisher](#)]
- [14]. Chen P., Shen J., Wang C., Wei Y., *Microchim. Acta*, 2018, **185**:113 [[Crossref](#)], [[Google Scholar](#)], [[Publisher](#)]
- [15]. Liu Y.M., Cao J.T., Zheng Y.L., Chen Y.H., *J. Sep. Sci.*, 2008, **31**:2463 [[Crossref](#)], [[Google Scholar](#)], [[Publisher](#)]
- [16]. Rezaei B., Ensafi A.A., Haghigatnia F., *Anal. Methods*, 2012, **4**:1573 [[Crossref](#)], [[Google Scholar](#)], [[Publisher](#)]
- [17]. Zhou M.X., Guan C.Y., Chen G., Xie X.Y., Wu S.H., *J. Zhejiang Univ. Sci. B*, 2005, **6**:1148 [[Crossref](#)], [[Google Scholar](#)], [[Publisher](#)]
- [18]. Liu P., Liu R., Guan G., Jiang C., Wang S., Zhang Z., *Analyst*, 2011, **136**:4152 [[Crossref](#)], [[Google Scholar](#)], [[Publisher](#)]
- [19]. Saka K., Uemura K., Shintani-Ishida K., Yoshida K.I., *J. Chromatogr. B*, 2007, **846**:240 [[Crossref](#)], [[Google Scholar](#)], [[Publisher](#)]
- [20]. Wong A., Santos A.M., Silva T.A., Fatibello-Filho O., *Talanta*, 2018, **183**:329 [[Crossref](#)], [[Google Scholar](#)], [[Publisher](#)]
- [21]. Mazloum-Ardakani M., Dehghani-Firouzabadi A., Sheikh-Mohseni M.A., Benvidi A., Mirjalili B.B.F., Zare R., *Measurement*, 2015, **62**:88 [[Crossref](#)], [[Google Scholar](#)], [[Publisher](#)]
- [22]. Bukkitgar S.D., Shetti N.P., *Mater. Today: Proceed.*, 2018, **5**:21474 [[Crossref](#)], [[Google Scholar](#)], [[Publisher](#)]
- [23]. Zhuang X., Chen D., Wang S., Liu H., Chen L., *Sens. Actuators B: Chem.*, 2017, **251**:185 [[Crossref](#)], [[Google Scholar](#)], [[Publisher](#)]
- [24]. Khodadadi A., Faghih-Mirzaei E., Karimi-Maleh H., Abbaspourrad A., Agarwal S., Gupta V.K., *Sens. Actuators B: Chem.* 2019, **284**:568 [[Crossref](#)], [[Google Scholar](#)], [[Publisher](#)]
- [25]. Shikandar D.B., Shetti N.P., Kulkarni R.M., Kulkarni S.D., *ECS J. Solid State Sci. Technol.*, 2018, **7**:Q3215 [[PDF](#)], [[Google Scholar](#)], [[Publisher](#)]
- [26]. Karimi-Maleh H., Orooji Y., Karimi F., Alizadeh M., Baghayeri M., Rouhi J., Tajik S., Beitollahi H., Agarwal S., Gupta V.K., Rajendran S., Ayati A., Fu L., Sanati A.L., Tanhaei B., Sen F., Shabani-Nooshabadi M., Naderi Asrami P., Al-Othman A., *Biosens. Bioelectron.*, 2021, **184**:113252 [[Crossref](#)], [[Google Scholar](#)], [[Publisher](#)]
- [27]. Tajik S., Beitollahi H., Garkani-Nejad F., Sheikhshoaei I., Sugih Nugraha A., Won Jang H., Yamauchi Y., Shokouhimehr M., *J. Mater. Chem. A*, 2021, **9**:8195 [[Crossref](#)], [[Google Scholar](#)], [[Publisher](#)]
- [28]. Karimi-Maleh H., Alizadeh M., Orooji Y., Karimi F., Baghayeri M., Rouhi J., Tajik S., Beitollahi H., Agarwal S., Gupta V.K., Rajendran S., Rostamnia S., Fu L., Saberi-Movahed F., Malekmohammadi S., *Ind. Eng. Chem. Res.*, 2021, **60**:816 [[Crossref](#)], [[Google Scholar](#)], [[Publisher](#)]
- [29]. Beitollahi H., Tajik S., Garkani-Nejad F., Safaei M., *J. Mater. Chem. B*, 2020, **8**:5826 [[Crossref](#)], [[Google Scholar](#)], [[Publisher](#)]
- [30]. Balasubramanian P., Settu R., Chen S.M., Chen T.W., *Microchim. Acta*, 2018, **185**:396 [[Crossref](#)], [[Google Scholar](#)], [[Publisher](#)]
- [31]. Karimi-Maleh H., Cellat K., Arikan K., Savk A., Karimi F., Şen F., *Mater. Chem. Phys.*, 2020, **250**:123042 [[Crossref](#)], [[Google Scholar](#)], [[Publisher](#)]
- [32]. Venu M., Venkateswarlu S., Reddy Y.V.M., Seshadri Reddy A., Gupta V.K., Yoon M., Madhavi G., *ACS Omega*, 2018, **3**:14597 [[Crossref](#)], [[Google Scholar](#)], [[Publisher](#)]
- [33]. Karimi-Maleh H., Karimi F., Malekmohammadi S., Zakariae N., Esmaeili R., Rostamnia S., Lütfi Yola M., Atar N., Movaghgharnezhad S., Rajendran S., Razmjou A., Orooji Y., Agarwal S., Gupta V.K., *J. Mol. Liq.*, 2020, **310**:113185 [[Crossref](#)], [[Google Scholar](#)], [[Publisher](#)]
- [34]. Huang Q., Lin X., Tong L., Tong Q.X., *ACS Sustain. Chem. Eng.* 2020, **8**:1644 [[Crossref](#)], [[Google Scholar](#)], [[Publisher](#)]

- [35]. Baghizadeh A., Karimi-Maleh H., Khoshnama Z., Hassankhani A., Abbasghorbani M., *Food Anal. Methods*, 2015, **8**:549 [[Crossref](#)], [[Google Scholar](#)], [[Publisher](#)]
- [36]. Garkani-Nejad F., Tajik S., Beitollahi H., Sheikhshoaei I., *Talanta*, 2021, **228**:122075 [[Crossref](#)], [[Google Scholar](#)], [[Publisher](#)]
- [37]. Karimi-Maleh H., Karimi F., Orooji Y., Mansouri G., Razmjou A., Aygun A., Sen F., *Sci. Rep.* 2020, **10**:11699 [[Crossref](#)], [[Google Scholar](#)], [[Publisher](#)]
- [38]. Alam, A. U.; Deen, M. J. *Anal.Chem.* 2020, **92**:5532 [[Crossref](#)], [[Google Scholar](#)], [[Publisher](#)]
- [39]. Karaman C., *Electroanalysis* 2021, **33**:1356 [[Crossref](#)], [[Google Scholar](#)], [[Publisher](#)]
- [40]. Akça A., Karaman O., Karaman C., *ECS J. Solid State Sci. Technol.* 2021, **10**:041003 [[Google Scholar](#)], [[Publisher](#)]
- [41]. Karaman C., Karaman O., Atar, N., Yola, M. L., *Electrochim. Acta*, 2021, **380**:138262 [[Crossref](#)], [[Google Scholar](#)], [[Publisher](#)]
- [42]. Karaman C., Karaman O., Yola B. B., Ulker İ., Atar N., Yola, M. L., *New J. Chem.* 2021, **45**:11222 [[Crossref](#)], [[Google Scholar](#)], [[Publisher](#)]
- [43]. Tajik S., Orooji Y., Ghazanfari Z., Karimi F., Beitollahi H., Varma RS., Jang HW., Shokouhimehr M., *J. Food Meas. Charact.*, 2021 [[Crossref](#)], [[Google Scholar](#)], [[Publisher](#)]
- [44]. Karaman C., Karaman O., Atar N., Yola, M. L., *Microchim. Acta* 2021, **188**:1 [[Crossref](#)], [[Google Scholar](#)], [[Publisher](#)]
- [45]. Karimi-Maleh H., Lütfi Yola M., Atar N., Orooji Y., Karimi F., Senthil Kumar P., Rouhi J., Baghayeri M., *J. Colloid Interface Sci.* 2021, **592**:174 [[Crossref](#)], [[Google Scholar](#)], [[Publisher](#)]
- [46]. Li Y.Y., Kang P., Wang S.Q., Liu Z.G., Li Y.X., Guo Z., *Sens. Actuators B: Chem.*, 2021, **327**:128878 [[Crossref](#)], [[Google Scholar](#)], [[Publisher](#)]
- [47]. Karimi-Maleh H., Sheikhshoaei M., Sheikhshoaei I., Ranjbar M., Alizadeh J., Maxakato N.W., Abbaspourrad A., *New J. Chem.*, 2019, **43**:2362 [[Crossref](#)], [[Google Scholar](#)], [[Publisher](#)]
- [48]. Orooji Y., Naderi Asrami P., Beitollahi H., Tajik S., Alizadeh M., Salmanpour S., Baghayeri M., Rouhi J., Sanati AL., Karimi F., J. *Food Meas. Charact.*, 2021 [[Crossref](#)], [[Google Scholar](#)], [[Publisher](#)]
- [49]. Miraki M., Karimi-Maleh H., Taher M.A., Cheraghi S., Karimi F., Agarwal S., Gupta V.K., *J. Mol. Liq.*, 2019, **278**:672 [[Crossref](#)], [[Google Scholar](#)], [[Publisher](#)]
- [50]. Tajik S., Beitollahi H., Won Jang H., Shokouhimehr M., *Talanta*, 2021, **232**:122379 [[Crossref](#)], [[Google Scholar](#)], [[Publisher](#)]
- [51]. Chen X., Pan H., Liu H., Dua M., *Electrochim. Acta*, 2010, **56**:636 [[Crossref](#)], [[Google Scholar](#)], [[Publisher](#)]
- [52]. Anuar N.S., Basirun W.J., Shalauddin M., Akhter S., *RSC Adv.*, 2020, **10**:17336 [[Crossref](#)], [[Google Scholar](#)], [[Publisher](#)]
- [53]. Wang M., Shi Y., Zhang Y., Wang Y., Huang H., Zhang J., Song J., *Electroanalysis*, 2017, **29**:2620 [[Crossref](#)], [[Google Scholar](#)], [[Publisher](#)]
- [54]. Wang W., Sun D., *Int. J. Electrochem. Sci.*, 2021, **16**:210216 [[Crossref](#)], [[Google Scholar](#)], [[Publisher](#)]
- [55]. Fayemi O.E., Adekunle A.S., Swamy B.K., Ebenso E.E., *J. Electroanal. Chem.*, 2018, **818**:236 [[Crossref](#)], [[Google Scholar](#)], [[Publisher](#)]
- [56]. Ding Z., Deng P., Wu Y., Tian Y., Li G., Liu J., He Q., *Molecules*, 2019, **24**:1178 [[Crossref](#)], [[Google Scholar](#)], [[Publisher](#)]
- [57]. Ni P., Sun Y., Shi Y., Dai H., Hu J., Wang Y., Li Z., *RSC Adv.*, 2014, **4**:28842 [[Crossref](#)], [[Google Scholar](#)], [[Publisher](#)]
- [58]. Song M.J., Hwang S.W., Whang D., *Talanta*, 2010, **80**:1648 [[Crossref](#)], [[Google Scholar](#)], [[Publisher](#)]
- [59]. Gou X., Sun S., Yang Q., Li P., Liang S., Zhang X., Yang Z., *New J. Chem.*, 2018, **42**:6364 [[Crossref](#)], [[Google Scholar](#)], [[Publisher](#)]
- [60]. Reitz E., Jia W., Gentile M., Wang Y., Lei Y., *Electroanalysis*, 2008, **20**:2482 [[Crossref](#)], [[Google Scholar](#)], [[Publisher](#)]
- [61]. Zhu G., Xu H., Xiao Y., Liu Y., Yuan A., Shen X., *ACS Appl. Mater. Interfaces*, 2012, **4**:744 [[Crossref](#)], [[Google Scholar](#)], [[Publisher](#)]
- [62]. Wang B., Wu X.L., Shu C.Y., Guo Y.G., Wang C.R., *J. Mater. Chem.*, 2010, **20**:10661 [[Crossref](#)], [[Google Scholar](#)], [[Publisher](#)]

- [63]. Zhuang Z., Su X., Yuan H., Sun Q., Xiao D., Choi M.M., *Analyst*, 2008, **133**:126 [[Crossref](#)], [[Google Scholar](#)], [[Publisher](#)]
- [64]. Bard A.J., Faulkner L.R., *Electrochemical Methods: Fundamentals and Applications*, John Wiley & Sons, New York, 2nd edn, 2001 [[PDF](#)], [[Google Scholar](#)]
- [65]. Mazloum-Ardakani M., Hosseinzadeh L., Khoshroo A., Naeimi H., Moradian M., *Electroanalysis* 2014, **26**:275 [[Crossref](#)], [[Google Scholar](#)], [[Publisher](#)]
- [66]. Keyvanfarad M., Alizad K. *Chin. J. Catal.* 2016, **37**:579 [[Crossref](#)], [[Google Scholar](#)], [[Publisher](#)]
- [67]. Kutluay A., Aslanoglu M. *J. Acta Chim. Slovenica*, 2010, **57**:157 [[Crossref](#)], [[Google Scholar](#)], [[Publisher](#)]

HOW TO CITE THIS ARTICLE

Abdolkazem neisi, Neda Kayedi, Parviz Mahmoudi. Identification of Filamentous Microorganisms Causing Filamentous Bulking and Factors Affecting Their Growth in a Petrochemical Wastewater Treatment Plant, *Chem. Methodol.*, 2021, 5(5) 397-406

DOI: 10.22034/chemm.2021.134961

URL: http://www.chemmethod.com/article_134961.html